Proceedings Paper:

Shen, Q., Liu, W. orcid.org/0000-0003-2968-2888, Wang, L. et al. (1 more author) (2019) Joint adaptive beamforming based on distributed moving platforms. In: 2018 IEEE 23rd International Conference on Digital Signal Processing (DSP). 2018 IEEE 23rd International Conference on Digital Signal Processing (DSP), 19-21 Nov 2018, Shanghai, China. IEEE .

https://doi.org/10.1109/ICDSP.2018.8631625

Joint Adaptive Beamforming Based on Distributed Moving Platforms

Qing Shen[†], Wei Liu[†*], Li Wang[‡*], Yin Liu[‡]
[†]Department of Electronic and Electrical Engineering, University of Sheffield
Sheffield, S1 3JD, United Kingdom
[‡]The 10th Research Institute of China Electronics Technology Group Corporation

***Abstract*—A distributed sensor array network consisting of sub-arrays with arbitrary locations and rotation angles placed on unmanned aerial vehicle (UAV) platforms is studied, where narrowband electro-magnetic waves are sent out by a transmitter, and the echo signals reflected from the targets are then received by the distributed UAV system. Based on this model, a joint reference signal based beamformer is proposed, leading to improved performance by exploiting the collected information across different sub-arrays simultaneously. Simulation results show that this novel beamformer is capable of extracting the signals of interest while suppressing interfering signals, and a lower mean square error (MSE) and higher output signal to interference plus noise ratio (SINR) are achieved compared with a regular reference signal based beamformer performed using a single sub-array.**

***Index Terms*—Adaptive beamforming, distributed sensor network, unmanned aerial vehicle (UAV), reference signal based beamformer.**

I. Introduction

To enhance the signals of interest (SOIs) from certain directions, adaptive beamformers (also known as spatial filters), which adjust their weight vector in a data-dependent manner to extract the SOIs while suppressing the interfering signals from other directions, play a very important role in various applications including wireless communications, radar, sonar, navigation, microphone array processing, and so on [1]–[3].

The linearly constrained minimum variance (LCMV) beamformer and the reference signal based (RSB) beamformer are two classes of well known beamformers [4]–[7]. With known or prior estimated direction of arrivals (DOAs) of the SOIs, the LCMV beamformers and their extensions [8], [9] offer improved robustness against inaccurate DOA estimates and sensor position errors by imposing constraints to the minimization problem of the output variance. For RSB beamformers [10], [11] where a reference signal is assumed to be available, adaptive beamforming is achieved by minimizing the mean square error (MSE) between the reference signal and the beamformer output. For adaptive beamformers [12]–[15], most of the adaptive algorithms employed are derived based on some stochastic gradient (SG) methods [16].

Traditionally, an adaptive beamformer is usually based on a single array with its sensors considered as part of a whole centred system, and distributed sensor arrays such as distributed microphone arrays [17], multistatic radar systems [18], and MIMO radars with widely separated antennas [19], [20] have attracted increasing attention in recent years.

In this paper, a distributed sensor array network consisting of sub-arrays based on unmanned aerial vehicle (UAV) platforms is first introduced, where the sub-array on each UAV may have an arbitrary rotation angle in the predefined Cartesian coordinate system, leading to different incident angles for different UAVs. Due to the extremely large spacing among the UAV platforms compared to half wavelength at the working frequency, SOIs received at different sub-arrays should not be considered as narrowband any more. Furthermore, since the UAVs may have unknown positions, velocities, moving directions, and rotation angles, the enhancement of the received SOIs by jointly exploiting information across all distributed sub-arrays is a very challenging problem. In this studied scenario, one transmitter sends out a known signal and it is then reflected back from the target and received by the distributed sensor array system. By considering the known transmitted signal as the reference signal, a joint reference signal based beamformer (JRSB) is then proposed to exploit the information acquired by all sub-arrays simultaneously, leading to improved performance compared with that of a regular RSB applied to a single UAV.

This paper is structured as follows. The distributed sensor array network with different sub-arrays carried by distributed UAV platforms is presented in Section II. The developed joint reference signal based beamformer (JRSB) is proposed in Section III. Simulation results are provided in Section IV, and conclusions are drawn in Section V.

II. System Model for Distributed UAV Platforms

Consider a distributed sensor array network consisting of M linear sub-arrays shown in Fig. 1, where each sub-array is fixed on a UAV platform, and $\mathrm{U}_m(x_m, y_m)$ represents the location of the m-th UAV in a predefined Cartesian coordinate system. A transmitter is employed to send out relatively narrowband (compared to the sub-array aperture) signal, and the echo signals reflected back from far-field targets together with the interferences from unknown directions are then received by the UAV-based sub-arrays.

Fig. 2(a) gives the general structure of the linear sub-array with L_m sensors placed on the m-th UAV. Assume that

*Corresponding authors: W. Liu and L. Wang

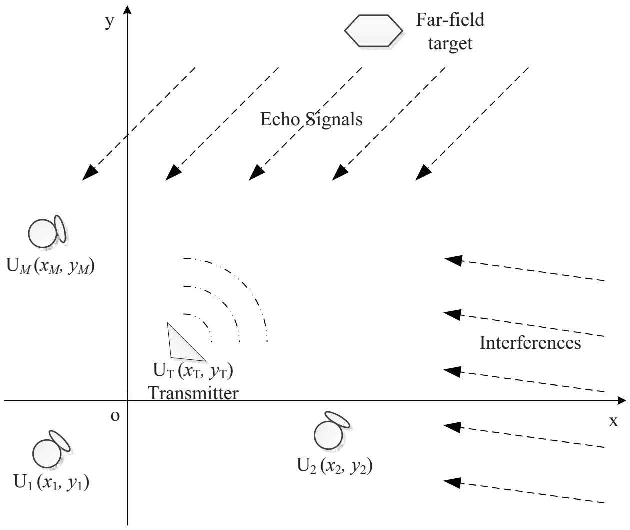

Fig. 1. A general model for a distributed sensor array system based on UAV platforms.

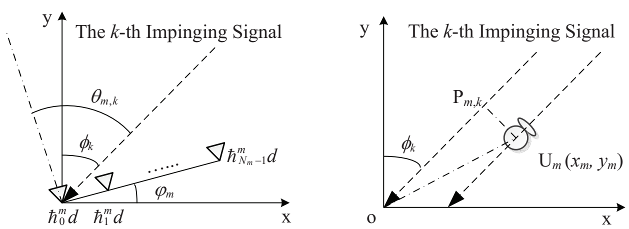

(a) The general array structure for the m-th UAV.

(b) The time delay.

Fig. 2. A general structure and the time delay for the m-th UAV.

there are K narrowband signals (including the echo signals and interferences) with incident angles ϕ_k, $k = 1, 2, \ldots, K$ (ϕ_k is measured between the direction of the signal and the y-axis of the Cartesian coordinate system). It is clear that $\theta_{m,k} = \phi_k + \varphi_m$, where the arbitrary rotation angle φ_m for the m-th sub-array is defined between the end-fire direction of the linear sub-array and the x-axis, while the incident angle $\theta_{m,k}$ of the k-th signal observed at the m-th sub-array is measured between the direction of the signal and the broadside of the array. The set of sensor positions for the m-th UAV is

$$\mathbb{S}_m = \left\{ \hbar^m_{l_m} d,\ 0 \leq l_m \leq L_m - 1, l_m \in \mathbb{Z} \right\} , \tag{1}$$

where $\mathbb{Z}$ is the set of all integers, and $d \leq \lambda/2$ is the unit spacing with λ being the signal wavelength.

Denote $\mathbf{x}_m(t)$ as the $L_M \times 1$ array observed signal vector, and the sub-array output model is given by

$$\mathbf{x}_m(t) = \mathbf{A}(\boldsymbol{\theta}_m, t)\mathbf{s}_m(t) + \bar{\mathbf{n}}_m(t) , \tag{2}$$

where $\mathbf{s}_m(t) = [s_{m,1}(t), s_{m,2}(t), \ldots, s_{m,K}(t)]^T$ represents the signal vector consisting of all the impinging signals with $\{\cdot\}^T$ denoting the transpose operation, $\bar{\mathbf{n}}_m(t)$ is the noise vector of the m-th sub-array, and $\mathbf{A}(\boldsymbol{\theta}_m, t) = [\mathbf{a}(\theta_{m,1}, t), \ldots, \mathbf{a}(\theta_{m,K}, t)]$ is the $L_m \times K$ steering matrix, with its k-th column vector $\mathbf{a}(\theta_{m,k}, t)$ being the steering vector corresponding to the k-th signal, expressed as

$$\mathbf{a}(\theta_{m,k}, t) = \left[a^m_{0,k}(t), a^m_{1,k}(t), \ldots, a^m_{L_m-1,k}(t) \right]^T , \tag{3}$$

with

$$a^m_{l_m,k}(t) = b^m_{l_m,k}(t) e^{-j\frac{2\pi\hbar^m_{l_m} d}{\lambda}\sin(\theta_{m,k})} , \tag{4}$$

where the reflection coefficient $b^m_{l_m,k}(t)$ of the k-th target corresponding to the l_m-th sensor of the m-th sub-array may be time-varying due to target motion or radar cross section (RCS) fluctuations, and it is assumed to be nearly unchanged in the observation time window.

Although the received signals are narrowband, the difference between those signals across sub-arrays from the same target can not be considered as a phase shift due to the much larger spacing between sub-arrays compared with the signal wavelength. As shown in Fig. 2(b), we take the origin $\mathrm{O}(0, 0)$ as the reference, and the angle $\angle\mathrm{XOU}_m$ between the x-axis and the direction from $\mathrm{O}(0, 0)$ to the m-th UAV position $\mathrm{U}_m(x_m, y_m)$ can be calculated by

$$\angle\mathrm{XOU}_m = \arctan 2(y_m, x_m) , \tag{5}$$

where $\arctan 2(y_m, x_m) \in (-\pi, \pi]$ returns the four-quadrant inverse tangent of y_m and x_m.

Then, we can obtain $R_{\mathrm{OU}_m} = \sqrt{x_m^2 + y_m^2}$ and angle $\angle\mathrm{P}_{m,k}\mathrm{OU}_m = \frac{\pi}{2} - \angle\mathrm{XOU}_m + \phi_k$, where R_{OU_m} is the distance between O and U_m. Therefore, we have $R_{\mathrm{OP}_{m,k}} = R_{\mathrm{OU}_m} \cdot \cos(\angle\mathrm{P}_{m,k}\mathrm{OU}_m)$, and the time delay between the origin and U_m is

$$\Delta\tau_{m,k} = -\frac{R_{\mathrm{OP}_{m,k}}}{c} = -\frac{\sqrt{x_m^2 + y_m^2} \cdot \cos(\angle\mathrm{P}_{m,k}\mathrm{OU}_m)}{c} , \tag{6}$$

where c is the wave propagation speed.

Denote $s_k(t)$, $k = 1, 2, \ldots, K$ as the k-th signal observed at the origin $\mathrm{O}(0, 0)$. Then the array output model of the m-th sub-array is updated to

$$\begin{aligned} \mathbf{x}_m(t) &= \mathbf{A}(\boldsymbol{\theta}_m, t)\mathbf{s}_m(t) + \bar{\mathbf{n}}_m(t) \\ &= \mathbf{A}(\boldsymbol{\theta}_m, t)\mathbf{s}(t - \boldsymbol{\tau}_m) + \bar{\mathbf{n}}_m(t) , \end{aligned} \tag{7}$$

where $\mathbf{s}(t - \boldsymbol{\tau}_m) = [s_1(t - \Delta\tau_{m,1}), \ldots, s_K(t - \Delta\tau_{m,K})]^T$.

III. Joint Reference Signal Based Beamformer for Distributed UAV Platforms

A. The Structure of the Proposed Beamformer

To exploit the information acquired by all sub-arrays simultaneously, a joint reference signal based beamformer (JRSB) is proposed with its structure after sampling with a frequency f_s given in Fig. 3, where $J - 1$ delay elements are allocated for each sensor channel with $T_s = 1/f_s$ being the time delay between adjacent taps of the tapped delay-lines, which are actually equivalent to a series of finite impulse response (FIR) filters. $x_{m,l_m}[n]$ is the signal received at the l_m-th sensor of the m-th sub-array, the reference signal $r[n]$ is a properly delayed copy of the known transmitted signal, and $\mathbf{w}_m[n] = \left[\{\mathbf{w}^m_0[n]\}^T, \{\mathbf{w}^m_1[n]\}^T, \ldots, \{\mathbf{w}^m_{J-1}[n]\}^T \right]^T$ is

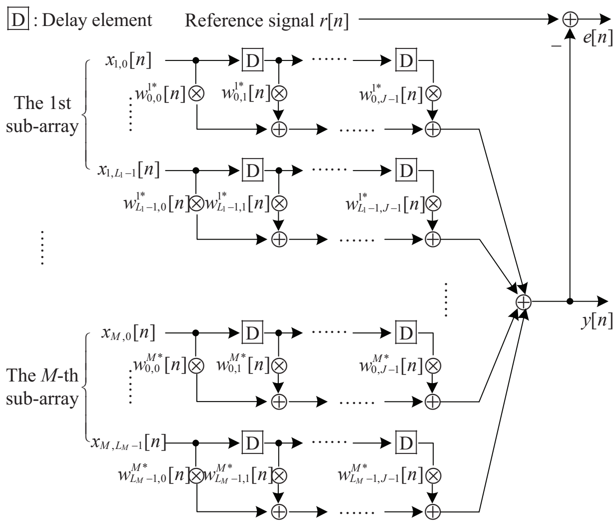

Fig. 3. A general structure of the proposed joint reference signal based beamformer.

the weight vector holding $L_m J$ complex coefficients, where each $\mathbf{w}_j^m[n] = \left[w_{0,j}^m[n], w_{1,j}^m[n], \ldots, w_{L_m-1,j}^m[n]\right]^T$, $j = 0, 1, \ldots, J-1$, and $\{\cdot\}^*$ is the complex conjugate operation.

Define $\tilde{\mathbf{x}}_m[n] = \left[\mathbf{x}_m^T[n], \mathbf{x}_m^T[n-1], \ldots, \mathbf{x}_m^T[n-(J-1)]\right]^T$ as the $L_m J \times 1$ observed signal vector. With $L = \sum_{m=1}^{M} L_m$, we construct an $LJ \times 1$ weight vector $\mathbf{w}[n]$ and an $LJ \times 1$ observed signal vector $\tilde{\mathbf{x}}[n]$ by

$$\begin{aligned} \mathbf{w}[n] &= \left[\mathbf{w}_1^T[n], \mathbf{w}_2^T[n], \ldots, \mathbf{w}_M^T[n]\right]^T \ . \\ \tilde{\mathbf{x}}[n] &= \left[\tilde{\mathbf{x}}_1^T[n], \tilde{\mathbf{x}}_2^T[n], \ldots, \tilde{\mathbf{x}}_M^T[n]\right]^T \ , \end{aligned} \tag{8}$$

Then, the beamformer output $y[n]$ is

$$y[n] = \mathbf{w}^H[n]\tilde{\mathbf{x}}[n] \ , \tag{9}$$

with $\{\cdot\}^T$ denoting the Hermitian transpose.

Finally, the error between the reference signal $r[n]$ and the output $y[n]$ is obtained by

$$\begin{aligned} e[n] &= r[n] - y[n] \\ &= r[n] - \mathbf{w}^H[n]\tilde{\mathbf{x}}[n] \ . \end{aligned} \tag{10}$$

B. Adaptive Algorithms for the Proposed Beamformer

Based on the proposed structure, the joint reference signal based beamformer can be constructed by employing all kinds of standard adaptive filtering algorithms, such as the least mean square (LMS) algorithm and the recursive least squares (RLS) algorithm [3]. In this paper, the Wiener solution basd on finite sample approximation and the normalized least mean square algorithm (NLMS) are employed for beamforming as representative examples. The cost function $\xi[n]$ at the time instant n, constructed by the mean square error (MSE), is formulated as

$$\begin{aligned} \xi[n] &= \mathrm{E}\left\{e[n]e^*[n]\right\} \\ &= \mathrm{E}\left\{(r[n] - \mathbf{w}^H[n]\tilde{\mathbf{x}}[n])(r[n] - \mathbf{w}^H[n]\tilde{\mathbf{x}}[n])^*\right\} \\ &= \sigma_r^2 - \mathbf{w}^H[n]\mathbf{p} - \mathbf{p}^H\mathbf{w}[n] + \mathbf{w}^H[n]\mathbf{R}_{\mathbf{xx}}\mathbf{w}[n] \ , \end{aligned} \tag{11}$$

where $\mathrm{E}\{\cdot\}$ is the expectation operation, $\sigma_r^2 = \mathrm{E}\left\{r[n]r^*[n]\right\}$ is the power of the reference signal, $\mathbf{p} = \mathrm{E}\left\{\tilde{\mathbf{x}}[n]r^*[n]\right\}$ is the cross-correlation vector between the received array signals and the reference signal, and $\mathbf{R}_{\mathbf{xx}} = \mathrm{E}\left\{\tilde{\mathbf{x}}[n]\tilde{\mathbf{x}}^H[n]\right\}$ is the covariance matrix of the received signals.

The gradient vector of the cost function $\xi[n]$ with respect to $\mathbf{w}^H[n]$ is given as

$$\nabla\xi[n] = -\mathbf{p} + \mathbf{R}_{\mathbf{xx}}\mathbf{w}[n] \ . \tag{12}$$

The optimum weight vector $\mathbf{w}_{\text{opt}}$ corresponding to the minimum MSE can be obtained by solving $\nabla\xi[n] = 0$, leading to the well-known Wiener solution [3], [16],

$$\mathbf{w}_{\text{opt}} = \mathbf{R}_{\mathbf{xx}}^{-1}\mathbf{p} \ . \tag{13}$$

In practice, the covariance matrix $\mathbf{R}_{\mathbf{xx}}$ and the cross-correlation vector $\mathbf{p}$ can be estimated by

$$\begin{aligned} \tilde{\mathbf{R}}_{\mathbf{xx}} &= \frac{1}{N}\sum_{n=0}^{N-1}\tilde{\mathbf{x}}[n]\tilde{\mathbf{x}}^H[n] \ , \\ \tilde{\mathbf{p}} &= \frac{1}{N}\sum_{n=0}^{N-1}\tilde{\mathbf{x}}[n]r^*[n] \ , \end{aligned} \tag{14}$$

where N is the number of data samples.

Then, by replacing $\mathbf{R}_{\mathbf{xx}}$ and $\mathbf{p}$ with the above sample covariance matrix $\tilde{\mathbf{R}}_{\mathbf{xx}}$ and sample cross-correlation vector $\tilde{\mathbf{p}}$, we can obtain the sample matrix inversion (SMI) solution based on finite sample approximation, given by

$$\mathbf{w}_{\text{SMI}} = \tilde{\mathbf{w}}_{\text{opt}} = \tilde{\mathbf{R}}_{\mathbf{xx}}^{-1}\tilde{\mathbf{p}} \ . \tag{15}$$

However, a sufficient number of data samples is required for accurate second-order statistics approximation, and the complexity of the SMI solution is extremely high due to the inverse operation.

To reduce the computational complexity, each of the expectation values can be simply replaced by an instantaneous single sample estimate based on $\tilde{\mathbf{x}}[n]$ and $r[n]$, i.e., $\hat{\mathbf{p}} = \tilde{\mathbf{x}}[n]r^*[n]$ and $\hat{\mathbf{R}}_{\mathbf{xx}} = \tilde{\mathbf{x}}[n]\tilde{\mathbf{x}}^H[n]$, and the gradient vector $\nabla\xi[n]$ is approximately

$$\nabla\xi[n] \approx -\hat{\mathbf{p}} + \hat{\mathbf{R}}_{\mathbf{xx}}\mathbf{w}[n] = -e^*[n]\tilde{\mathbf{x}}[n] \ . \tag{16}$$

Then, we can update the weight vector $\mathbf{w}[n]$ with each new data sample in the negative direction of the gradient with a step size μ_0, leading to the least mean square (LMS) algorithm, shown as

$$\mathbf{w}[n+1] = \mathbf{w}[n] + \mu_0 e^*[n]\tilde{\mathbf{x}}[n] \ , \tag{17}$$

where the step size μ_0 is a positive real-valued constant weighting the amount of innovation applied at each step, and it can be normalized in a data dependent manner to ensure an approximately constant rate of adaptation by defining

$$\mu_0 = \frac{\mu}{\tilde{\mathbf{x}}^H[n]\tilde{\mathbf{x}}[n]} \ . \tag{18}$$

Then, the resultant normalized least mean square algorithm (NLMS) can be expressed as

$$\mathbf{w}[n+1] = \mathbf{w}[n] + \frac{\mu}{\tilde{\mathbf{x}}^H[n]\tilde{\mathbf{x}}[n]} e^*[n]\tilde{\mathbf{x}}[n] \; , \tag{19}$$

where we normally choose $0 < \mu < 0.5$ to ensure stability of the NLMS algorithm.

IV. Simulation Results

Consider $M = 3$ sub-arrays carried on three UAV platforms. Each sub-array is a uniform linear array with $L_m = 6$ sensors, $\forall m = 1, 2, 3$, and the unit spacing $d = \lambda/2$. The positions of the three sub-arrays are $\mathrm{U}_1(0, -40)$, $\mathrm{U}_2(25, 20)$, and $\mathrm{U}_3(-60, 70)$, while their rotation angles are $55°$, $30°$, and $-20°$, respectively. The reference signal is adjusted with a proper time delay compared to the transmitted signal according to a coarse estimation of the target range of interest. For the far-field targets, the reflection coefficients $b^m_{l_m,k}(t)$ are randomly generated constant complex values sharing the same amplitude for all sensors. We set the signal to noise ratio (SNR) to 20dB, $J = 80$, and $\mu = 0.1$. The working frequency is 10 GHz and the signal propagation speed $c = 3 \times 10^8$ m/s with the signal wavelength $\lambda = 0.03$m. The spacings among the UAV platforms are 65.00m, 98.62m, and 125.30m, respectively, and all of them are extremely larger than the signal wavelength. Note that these information are unknown for the beamformers.

In the first scenario, there are $K = 3$ impinging signals with one far-field target coming from $-10°$, while the incident angles of the two interferences are $-30°$ and $20°$, respectively. The signal to interference ratio (SIR) for each interfering signal is 0dB. Then, we focus on the ensemble mean square error (MSE) results of $e[n]$ with respect to the number of samples, defined as

$$\mathrm{EMSE}[n] = \sqrt{\frac{1}{Q}\sum\nolimits_{q=1}^{Q} |\hat{e}_q[n]|^2} \; , \tag{20}$$

where Q is the number of independent simulation runs, and $\hat{e}_q[n]$ is the error at iteration number n of the q-th trial.

Fig. 4(a) gives the ensemble MSE results for different beamformers based on $Q = 500$ Monte Carlo simulation trials, where the NLMS JRSB represents the proposed JRSB using the NLMS algorithm, the SMI JRSB is the proposed JRSB employing the SMI solution, and the regular NLMS RSB represents the RSB using the NLMS algorithm based on a single sub-array located at $\mathrm{U}_1(0, -40)$ with a rotation angle $55°$. Obviously, both the NLMS JRSB and the SMI JRSB provide a much faster convergence speed as well as lower MSEs than the regular one. Furthermore, the SMI JRSB provides the best results for a sufficient number of samples involved. It is noted that $\tilde{\mathbf{R}}_{\mathbf{xx}}$ is a matrix with a size of 1440×1440, and there exists serious degradation in the performance of the SMI JRSB for a small number of samples less than 1000 due to worse approximations to the second-order statistics.

The output signal to interference plus noise ratio (SINR) of different beamformers are shown in Fig. 4(b). It is clear that the output SINR of the regular NLMS RSB is the worst among the three beamformers, while the output SINR of the two JRSBs are close to each other with that of the SMI JRSB a bit higher, which is consistent with the ensemble MSE results in Fig. 4(a).

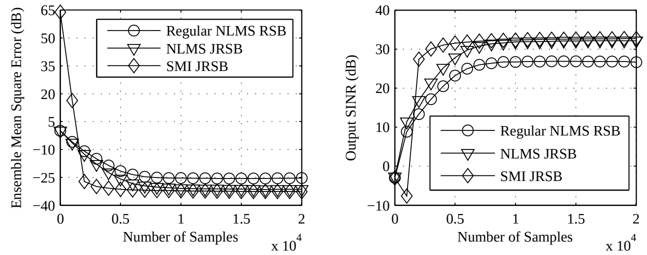

(a) Ensemble MSE. (b) Output SINR.

Fig. 4. Ensemble MSE and Output SINR of different beamformers for $K = 3$ with one target.

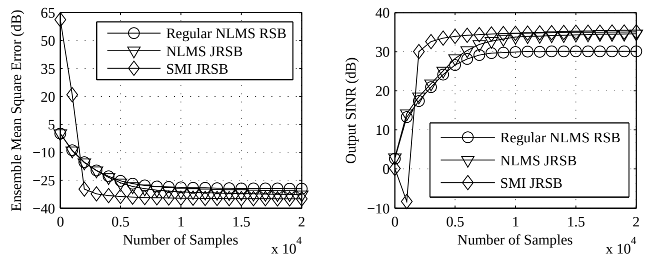

(a) Ensemble MSE. (b) Output SINR.

Fig. 5. Ensemble MSE and Output SINR of different beamformers for $K = 4$ with two targets.

In the second scenario, we add another far-field target with incident angle of $-50°$, and other settings remain the same as the first scenario. Now there are $K = 4$ impinging signals with two being of interest. The ensemble MSE results and the output SINR of different beamformers are shown in Figs. 5(a) and 5(b), respectively, which again verify the superior performance of the proposed NLMS JRSB and SMI JRSB.

V. Conclusions

In this paper, a distributed sensor array network consisting of sub-arrays placed on UAV platforms has been studied, where arbitrary locations and rotation angles are allocated to each UAV-based sub-array. In this studied model, a transmitter is used to send out a single signal while the echo signals reflected from far-field targets are then received by the distributed sensor array system. To enhance the SOIs while suppressing interfering signals, a joint reference signal based beamformer (JRSB) was proposed to exploit the information acquired by all the sub-arrays, where the NLMS algorithm and sample matrix inversion (SMI) solution based on finite sample approximation are employed for adaptive beamforming. It has been shown by simulations that the proposed JRSB offers a much better performance than the regular beamformer applied to a single sub-array.

REFERENCES

[1] H. Krim and M. Viberg, "Two decades of array signal processing research: the parametric approach," *IEEE Signal Processing Magazine*, vol. 13, no. 4, pp. 67–94, July 1996.

[2] B. Allen and M. Ghavami, *Adaptive Array Systems, Fundamentals and Applications*. Chichester, England: John Wiley & Sons, 2005.

[3] W. Liu and S. Weiss, *Wideband Beamforming: Concepts and Techniques*. Chichester, UK: John Wiley & Sons, 2010.

[4] J. Capon, "High-resolution frequency-wavenumber spectrum analysis," *Proc. IEEE*, vol. 57, no. 8, pp. 1408–1418, Aug. 1969.

[5] B. D. Van Veen and K. M. Buckley, "Beamforming: a versatile approach to spatial filtering," *IEEE Acoustics, Speech, and Signal Processing Magazine*, vol. 5, no. 2, pp. 4–24, April 1988.

[6] B. Breed and J. Strauss, "A short proof of the equivalence of lcmv and gsc beamforming," *IEEE Signal Processing Letters*, vol. 9, pp. 168–169, June 2002.

[7] R. C. de Lamare and R. Sampaio-Neto, "Low-complexity variable step-size mechanisms for stochastic gradient algorithms in minimum variance cdma receivers," *IEEE Trans. Signal Process.*, vol. 54, no. 6, pp. 2302–2317, 2006.

[8] R. C. de Lamare, L. Wang, and R. Fa, "Adaptive reduced-rank lcmv beamforming algorithms based on joint iterative optimization of filters: Design and analysis," *Signal Processing*, vol. 90, no. 2, pp. 640–652, 2010.

[9] J. Xu, G. Liao, S. Zhu, and L. Huang, "Response vector constrained robust lcmv beamforming based on semidefinite programming," *IEEE Trans. Signal Process.*, vol. 63, no. 21, pp. 5720–5732, 2015.

[10] L. Zhang, W. Liu, and R. J. Langley, "A class of constrained adaptive beamforming algorithms based on uniform linear arrays," *IEEE Transactions on Signal Processing*, vol. 58, no. 7, pp. 3916–3922, July 2010.

[11] L. Zhang, W. Liu, A. ul Quddus, M. Dianati, and R. Tafazolli, "Adaptive distributed beamforming for relay networks based on local channel state information," *IEEE Transactions on Signal and Information Processing over Networks*, vol. 1, no. 2, pp. 117–128, 2015.

[12] Y. Zhao, W. Liu, and R. J. Langley, "Adaptive wideband beamforming with frequency invariance constraints," *IEEE Transactions on Antennas and Propagation*, vol. 59, no. 4, pp. 1175–1184, April 2011.

[13] M. B. Hawes and W. Liu, "Sparse array design for wideband beamforming with reduced complexity in tapped delay-lines," *IEEE/ACM Trans. Audio, Speech, Language Process.*, vol. 22, no. 8, pp. 1236–1247, Aug. 2014.

[14] Y. Bao and H. Chen, "Design of robust broadband beamformers using worst-case performance optimization: A semidefinite programming approach," *IEEE/ACM Trans. Audio, Speech, Language Process.*, vol. 25, no. 4, pp. 895–907, Apr. 2017.

[15] M. R. Anbiyaei, W. Liu, and D. C. McLernon, "Performance improvement for wideband beamforming with white noise reduction based on sparse arrays," in *Proc. European Signal Processing Conference (EUSIPCO)*, 2017, pp. 2433–2437.

[16] S. Haykin, *Adaptive Filter Theory*, 3rd ed. Englewood Cliffs, New York: Prentice Hall, 1996.

[17] K. Imoto and N. Ono, "Spatial cepstrum as a spatial feature using a distributed microphone array for acoustic scene analysis," *IEEE/ACM Trans. Audio, Speech, Language Process.*, vol. 25, no. 6, pp. 1335–1343, 2017.

[18] X. Zhang, H. Li, and B. Himed, "Multistatic passive detection with parametric modeling of the io waveform," *Signal Processing*, vol. 141, pp. 187–198, 2017.

[19] A. A. Gorji, R. Tharmarasa, and T. Kirubarajan, "Widely separated MIMO versus multistatic radars for target localization and tracking," *IEEE Trans. Aerosp. Electron. Syst.*, vol. 49, no. 4, pp. 2179–2194, 2013.

[20] A. M. Haimovich, R. S. Blum, and L. J. Cimini, "MIMO radar with widely separated antennas," *IEEE Signal Process. Mag.*, vol. 25, no. 1, pp. 116–129, 2008.